European Heart Journal (2015) **36**, 806–816
doi:10.1093/eurheartj/ehu411

**BASIC SCIENCE**

# Pravastatin reverses obesity-induced dysfunction of induced pluripotent stem cell-derived endothelial cells via a nitric oxide-dependent mechanism

**Mingxia Gu[1,2,3†], Nicholas M. Mordwinkin[1,2,3†], Nigel G. Kooreman[1,2,3,4], Jaecheol Lee[1,2,3], Haodi Wu[1,2,3], Shijun Hu[1,2,3], Jared M. Churko[1,2,3], Sebastian Diecke[1,2,3], Paul W. Burridge[1,2,3], Chunjiang He[1,2,3], Frances E. Barron[1,2,3], Sang-Ging Ong[1,2,3], Joseph D. Gold[1], and Joseph C. Wu[1,2,3*]**

[1]Stanford Cardiovascular Institute, Stanford University School of Medicine, Stanford, CA, USA; [2]Institute for Stem Cell Biology and Regenerative Medicine, Stanford University School of Medicine, Stanford, CA, USA; [3]Division of Cardiology, Department of Medicine, Stanford University School of Medicine, Stanford, CA, USA; and [4]Department of Vascular Surgery, Leiden University Medical Center, Leiden, The Netherlands

*Received 10 February 2014; revised 17 September 2014; accepted 23 September 2014; online publish-ahead-of-print 27 February 2014*

**Aims** High-fat diet-induced obesity (DIO) is a major contributor to type II diabetes and micro- and macro-vascular complications leading to peripheral vascular disease (PVD). Metabolic abnormalities of induced pluripotent stem cell-derived endothelial cells (iPSC-ECs) from obese individuals could potentially limit their therapeutic efficacy for PVD. The aim of this study was to compare the function of iPSC-ECs from normal and DIO mice using comprehensive *in vitro* and *in vivo* assays.

**Methods and results** Six-week-old C57Bl/6 mice were fed with a normal or high-fat diet. At 24 weeks, iPSCs were generated from tail tip fibroblasts and differentiated into iPSC-ECs using a directed monolayer approach. *In vitro* functional analysis revealed that iPSC-ECs from DIO mice had significantly decreased capacity to form capillary-like networks, diminished migration, and lower proliferation. Microarray and ELISA confirmed elevated apoptotic, inflammatory, and oxidative stress pathways in DIO iPSC-ECs. Following hindlimb ischaemia, mice receiving intramuscular injections of DIO iPSC-ECs had significantly decreased reperfusion compared with mice injected with control healthy iPSC-ECs. Hindlimb sections revealed increased muscle atrophy and presence of inflammatory cells in mice receiving DIO iPSC-ECs. When pravastatin was co-administered to mice receiving DIO iPSC-ECs, a significant increase in reperfusion was observed; however, this beneficial effect was blunted by co-administration of the nitric oxide synthase inhibitor, $N^{\omega}$-nitro-L-arginine methyl ester.

**Conclusion** This is the first study to provide evidence that iPSC-ECs from DIO mice exhibit signs of endothelial dysfunction and have suboptimal efficacy following transplantation in a hindlimb ischaemia model. These findings may have important implications for future treatment of PVD using iPSC-ECs in the obese population.

**Keywords** Diet-induced obesity • Induced pluripotent stem cells • Endothelial cells • Hindlimb ischaemia • Statins • Peripheral vascular disease

* Corresponding author. 265 Campus Drive, G1120B, Stanford, CA 94305-5454, USA. Tel: +1 650 736 2246, Fax: +1 650 736 0234, Email: joewu@stanford.edu

† These authors contributed equally to this work.

## Translational perspective

This study investigates the hypothesis that iPSC-ECs derived from diet-induced obesity (DIO) mice will exhibit signs of endothelial dysfunction and may not be suitable for therapeutic transplantation in a hindlimb ischaemia model. We also explore the use of statins to reverse endothelial dysfunction both *in vitro* and *in vivo*.

# Introduction

Obesity is a rapidly growing threat to global healthcare, with >1.5 billion adults overweight and 400 million of them considered obese. Increasing evidence indicates a high-caloric high-fat diet is a significant risk factor for causing deleterious effects on metabolism and heart function, and has been strongly linked to the progression of heart disease and type 2 diabetes.[1–3] Dysglycaemia associated with obesity, insulin resistance and subsequent diabetes mellitus can lead to decreased nitric oxide (NO) bioavailability, endothelial nitric oxide synthase (eNOS) uncoupling, and increased levels of reactive oxygen species (ROS).[4] Left unchecked, this oxidative stress can result in an increased production of pro-inflammatory cytokines, leading to oxidative DNA damage and the activation of cellular apoptotic signals and pathways.[5,6] The hallmark of endothelial dysfunction involved in obesity and its vascular complications is thought to be the result of interplay between apoptosis, inflammation, and oxidative stress, including a reduced bioavailability of NO.[7] Statins are 3-hydroxy-3-methyl-glutaryl-CoA reductase inhibitors used primarily to lower cholesterol levels. Statins have also been shown to have beneficial effects on endothelial progenitor cells, improve endothelial function, increase NO production, augment neovascularization, and decrease ROS and inflammatory cytokines.[8]

In recent years, embryonic stem cell-derived endothelial cells (ESC-ECs) have been evaluated in models of myocardial infarction and hindlimb ischaemia as a potential therapeutic option to promote angiogenesis and neovascularization.[9–11] At present, therapies derived from ESCs are associated with significant ethical and political concerns. The recent discovery of induced pluripotent stem cells (iPSCs) has provided an alternative for the treatment of ischaemic vascular disease.[12] However, little is known about the function of induced pluripotent stem cell-derived endothelial cells (iPSC-ECs) derived from obese or overweight individuals, specifically whether they exhibit properties of endothelial dysfunction and impaired vascular function similar to native ECs from these individuals. This could potentially limit the use of iPSC-ECs from patients with diabetes as a therapeutic option for peripheral vascular disease (PVD) unless co-administer with low-dose pravastatin therapy.

# Methods

An extended methods section is available in Supplementary material online.

## Surgical model for hindlimb ischaemia and cell delivery

The surgical procedure for the induction of unilateral hindlimb ischaemia was performed following a previously published protocol.[13] Briefly, mice were anesthetized in an induction chamber containing 1–2% isoflurane (Baxter HealthCare, Deerfield, IL, USA) in 100% oxygen at a flow rate of 1 L/min. Ischaemia was induced by two separate ligations of the femoral artery, one distal and one proximal to the origin of the deep femoral branch. Subsequently, the skin was closed using 5-0 Vicryl sutures. Following the operation, animals were randomized into seven groups ($n = 10$ per group) and each was administered a single gastrocnemius intramuscular (IM) injection containing: (i) 50 μL of 1 : 1 Matrigel/EBM2 (vehicle), (ii) vehicle plus intraperitoneal (IP) pravastatin co-administration daily, (iii) $1 \times 10^6$ pooled iPSC-ECs from control donors in 50 μL of 1 : 1 Matrigel/EBM2, (iv) $1 \times 10^6$ pooled iPSC-ECs from DIO donors in 50 μL of 1 : 1 Matrigel/EBM2, (v) a single injection of $1 \times 10^6$ pooled iPSC-ECs from DIO donors plus co-administration of pravastatin (20 mg/kg body weight; injected volume, 0.02 mL/g body weight, IP), (vi) a single injection of $1 \times 10^6$ pooled iPSC-ECs from DIO donors pre-incubated with 1 μM pravastatin for 7 days, and (vii) a single injection of $1 \times 10^6$ pooled iPSC-ECs from DIO donors plus co-administration of pravastatin and NO synthase inhibitor $N^{\omega}$-nitro-L-arginine methyl ester (L-NAME) daily. Prior to cell injection, iPSC-ECs were labelled with CellTracker CM-DiI cell-labelling solution (Life Technologies) according to the manufacturer's instructions so that the injected cells could be visualized post-mortem.[14] To inhibit NO synthesis, L-NAME was administered in the drinking water at a concentration of 1 mg/mL during days 1 through 14 post cell delivery. Laser Doppler imaging (LDI) was performed on Days 0, 3, 7, 10, and 14 following cell injection.

## Statistical analysis

Statistics were calculated using GraphPad Prism (GraphPad Software, La Jolla, CA, USA). *In vitro* data were obtained from at least three independent experiments. Statistical significance between two groups was determined by paired or unpaired Student's *t*-test. For simple comparison between groups, one-way ANOVA was applied if the data were normally distributed, otherwise nonparametric Kruskal–Wallis test was used. For drug treatment experiments, two-way ANOVA followed by Bonferroni or Tukey's *post hoc* tests were applied. *P*-values were considered statistically significant if $P < 0.05$ and all actual *P*-value are shown in the figures. All data are expressed as mean ± SD.

# Results

## Reprogramming of fibroblasts from control and diet-induced obesity mice into induced pluripotent stem cells

A previously published study has demonstrated that iPSCs can be generated from individuals with type 1 diabetes.[15] However, this study did not report the reprogramming efficiency of these cells. Hence, to test whether there is an inherent difference in the capacity of fibroblasts from control and DIO mice to be reprogrammed into iPSCs, tail tip fibroblasts were isolated from 24-week-old C57Bl/6 mice fed either a normal (10 kcal% from fat) or high-fat (60 kcal% from fat) diet beginning at 6 weeks of age. At 24 weeks of age, high-fat DIO mice had significantly increased body weight ($P = 0.001$), fasting glucose ($P = 0.016$), and showed a significant decrease in glucose and insulin tolerance compared to control mice ($P < 0.0001$; Supplementary material

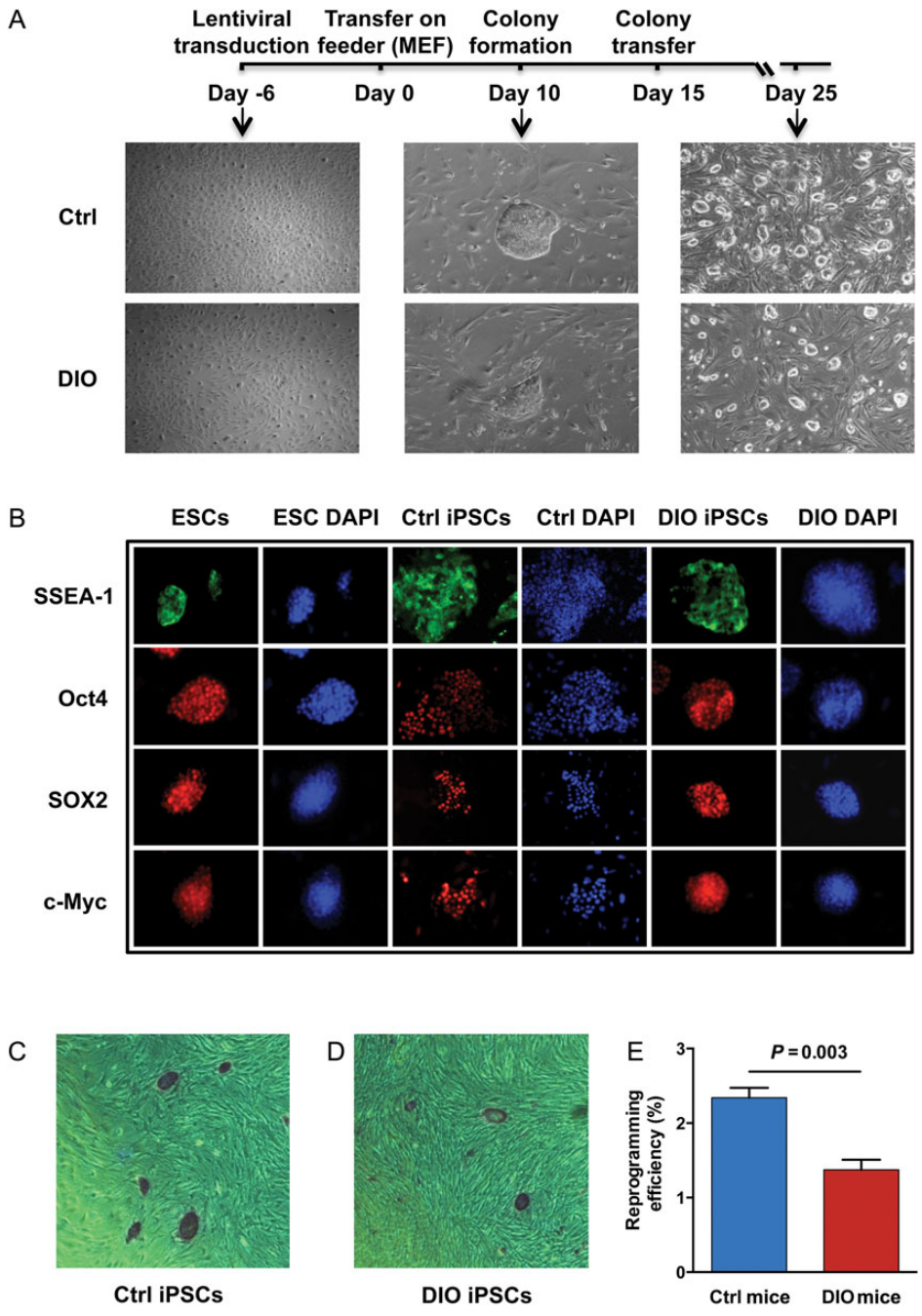


**Figure 1** Generation and characterization of induced pluripotent stem cells. (*A*) Representative timeline of murine induced pluripotent stem cell generation. (*B*) Immunofluorescence of pluripotency markers SSEA-1, Oct4, Sox2, and c-Myc in mouse induced pluripotent stem cells. Mouse embryonic stem cells were used as positive control. (*C*–*E*) All murine induced pluripotent stem cell colonies stained positive for alkaline phosphatase. Reprogramming efficiency was significantly lower in induced pluripotent stem cells derived from diet-induced obesity tail tip fibroblasts compared with those derived from control mice ($n = 5$/group, $P = 0.003$).

online, *Figure S1A–D*). Next, we successfully reprogrammed tail tip fibroblasts into murine iPSCs using a codon optimized 4-in-1 lentiviral vector encoding *Oct-4*, *Klf4*, *Sox2*, and *c-Myc*. On Day 15 after reprogramming, we mechanically dissociated the individual iPSC colonies and transferred them onto irradiated MEF feeder layers for clonal expansion into multiple cell lines (3 lines/mouse, 5 mice/group) (*Figure 1A*). All murine iPSC colonies stained positive for alkaline phosphatase, as well as pluripotency markers SSEA-1, Oct4, Sox2, and c-Myc (*Figure 1B–D*). Interestingly, reprogramming efficiency was significantly lower in iPSCs derived from DIO mice compared with those derived from control mice ($P = 0.003$; *Figure 1E*). Immunohistochemistry and real-time

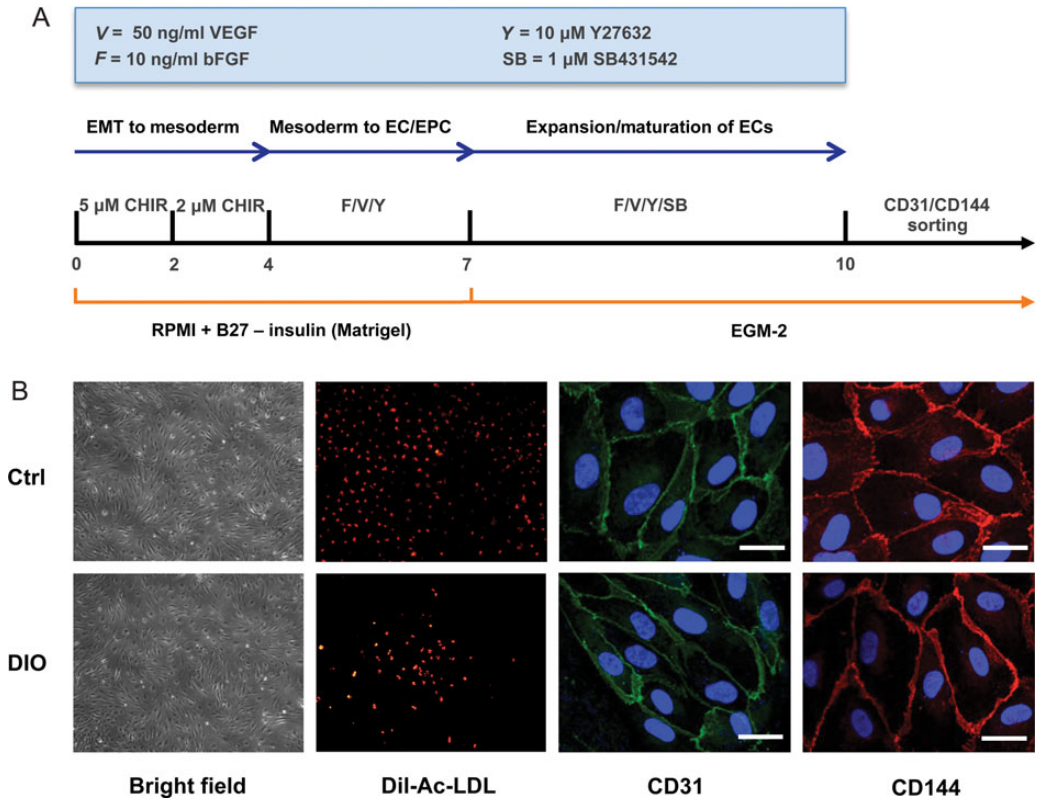


**Figure 2** Differentiation of induced pluripotent stem cells into induced pluripotent stem cell-derived endothelial cells. (*A*) An outline of the protocol used for the differentiation of murine induced pluripotent stem cells to induced pluripotent stem cell-derived endothelial cells. At Day 14, induced pluripotent stem cell-derived endothelial cells were stained for CD31 and CD144, and double-positive ($CD31^+/CD144^+$) cells were expanded on 0.2% gelatin-coated plates in EGM-2 medium. (*B*) Representative brightfield images and positive immunofluorescence of differentiated induced pluripotent stem cell-derived endothelial cells for CD31 and CD144 at 63×. Differentiated induced pluripotent stem cell-derived endothelial cells also exhibited DiI-Ac-LDL uptake.

polymerase chain reaction (RT-PCR) confirmed that the established iPSC lines were able to form cells derived from all three germ layers *in vitro*, expressed markers specific for endoderm, ectoderm, and mesoderm (Supplementary material online, *Figure S2A* and *B* and *Table S1*), and also maintained a normal karyotype after extended passage (Supplementary material online, *Figure S3A* and *B*).

## Control and diet-induced obesity induced pluripotent stem cells can be successfully differentiated into induced pluripotent stem cell-derived endothelial cells

Next, we successfully differentiated iPSCs (at passage 15) from control and DIO mice into iPSC-ECs via a chemically defined monolayer differentiation protocol (*Figure 2A*). On Day 10 after induction of differentiation, iPSC-ECs were stained using antibodies against CD31 and CD144 and subsequently sorted by FACS. Double-positive ($CD31^+/CD144^+$) cells were then plated on 0.2% gelatin-coated plates for further expansion and characterization. Isolated iPSC-ECs showed DiI-Ac-LDL uptake and stained positive for endothelial markers CD31 and CD144 (*Figure 2B*). Flow cytometry showed no significant difference in EC differentiation capacity between iPSCs generated from DIO mice or healthy mice (18.80 ± 1.51% vs. 20.47 ± 1.75%, respectively; $P = 0.28$) (Supplementary material online, *Figure S4*).

## Diet-induced obesity induced pluripotent stem cell-derived endothelial cells exhibit endothelial dysfunction phenotype *in vitro*

Endothelial cells isolated from obese individuals have been shown to demonstrate properties of endothelial dysfunction *in vitro*.[16] Similarly, we found cell migration and proliferation were significantly reduced among both aortic-ECs (data not shown) and iPSC-ECs from DIO mice compared with aortic-ECs and iPSC-ECs from control mice ($P < 0.05$; *Figure 3A*, *B* and *E*). Additionally, iPSC-ECs from DIO but not control mice showed a significant increase in apoptosis when cultured in a hypoxic environment ($P = 0.007$; *Figure 3C* and *D*). iPSC-ECs from DIO mice had significantly reduced capacity to form cord-like structures on Matrigel compared with control cells after 24 h ($P < 0.001$; *Figure 3F*). Incubation of iPSC-ECs from DIO mice with 1 μM pravastatin for 24 h resulted in significant increases in cell migration ($P < 0.001$), proliferation ($P = 0.003$), and number of cord-like structures on Matrigel ($P < 0.001$), and significant decrease

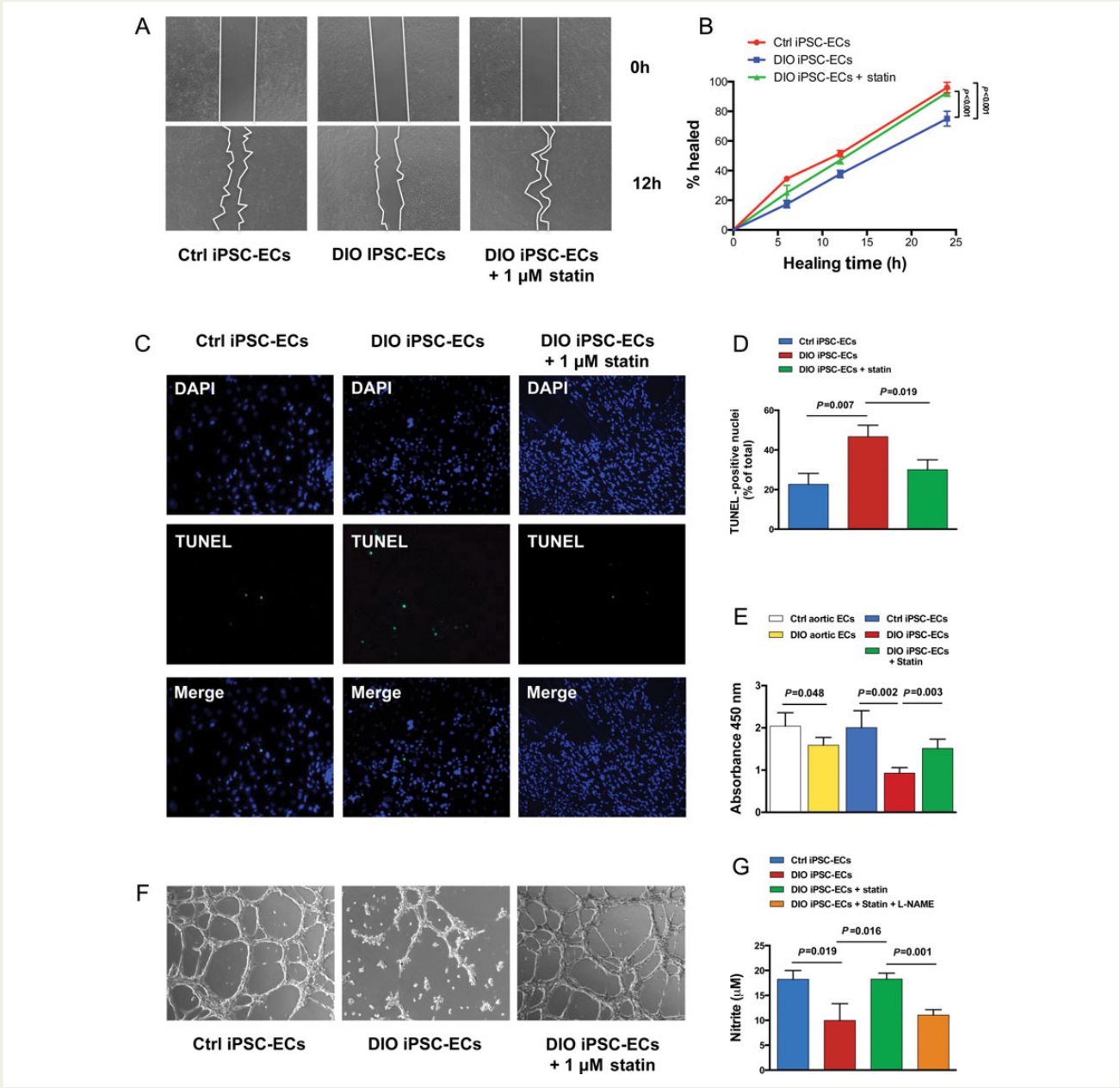


**Figure 3** Characterization of induced pluripotent stem cell-derived endothelial cells *in vitro*. (*A* and *B*) Induced pluripotent stem cell-derived endothelial cells from diet-induced obesity mice demonstrated significant reduction in cell migration ($P < 0.001$). (*C* and *D*) TUNEL staining of diet-induced obesity induced pluripotent stem cell-derived endothelial cells demonstrated significant increase in apoptosis compared with control induced pluripotent stem cell-derived endothelial cells when cultured in hypoxic conditions ($P = 0.007$). (*E*) Both aortic-endothelial cells and induced pluripotent stem cell-derived endothelial cells from diet-induced obesity mice showed significant decrease in cell proliferation compared with control mice ($P = 0.048$ in aortic endothelial cells; $P = 0.002$ in induced pluripotent stem cell-derived endothelial cells). (*F*) Diet-induced obesity induced pluripotent stem cell-derived endothelial cells also demonstrated a reduced capacity to form cord-like network on Matrigel after 24 h compared with control induced pluripotent stem cell-derived endothelial cells ($P < 0.001$). The addition of 1 μM pravastatin to diet-induced obesity induced pluripotent stem cell-derived endothelial cells for 24 h resulted in significant increases in cell migration ($P < 0.001$), proliferation ($P = 0.003$), and the number of cord-like structures ($P < 0.001$), while significantly decreasing endothelial cell apoptosis ($P = 0.019$). (*G*) Measurement of nitrite levels in cell culture supernatant by Griess reaction demonstrated that diet-induced obesity induced pluripotent stem cell-derived endothelial cells had significantly lower levels of nitric oxide production compared with control induced pluripotent stem cell-derived endothelial cells ($P = 0.019$). Incubation of diet-induced obesity induced pluripotent stem cell-derived endothelial cells with 1 μM pravastatin for 24 h resulted in significantly higher levels of nitric oxide ($P = 0.016$). The effect of pravastatin on nitrite levels in diet-induced obesity induced pluripotent stem cell-derived endothelial cell was blocked by co-incubation with $N^{\omega}$-nitro-L-arginine methyl ester ($P = 0.001$).

in apoptosis ($P = 0.019$). Finally, DIO iPSC-ECs had significantly lower levels of NO production compared with control iPSC-ECs ($P = 0.019$); incubation of DIO iPSC-ECs with 1 μM pravastatin for 24 h resulted in significantly higher levels of NO ($P = 0.016$). However, the effect of pravastatin in DIO iPSC-ECs was blocked by co-incubation with the NO synthase inhibitor L-NAME ($P = 0.001$) (*Figure 3G*). Interestingly, incubation of DIO iPSC-ECs with other statins including rosuvastatin (R-statin) and atorvastatin (A-statin) resulted in much less functional recovery compared with pravastatin (P-statin) (Supplementary material online, *Figure S5*), which might be due to their different pharmacokinetic properties.[17]

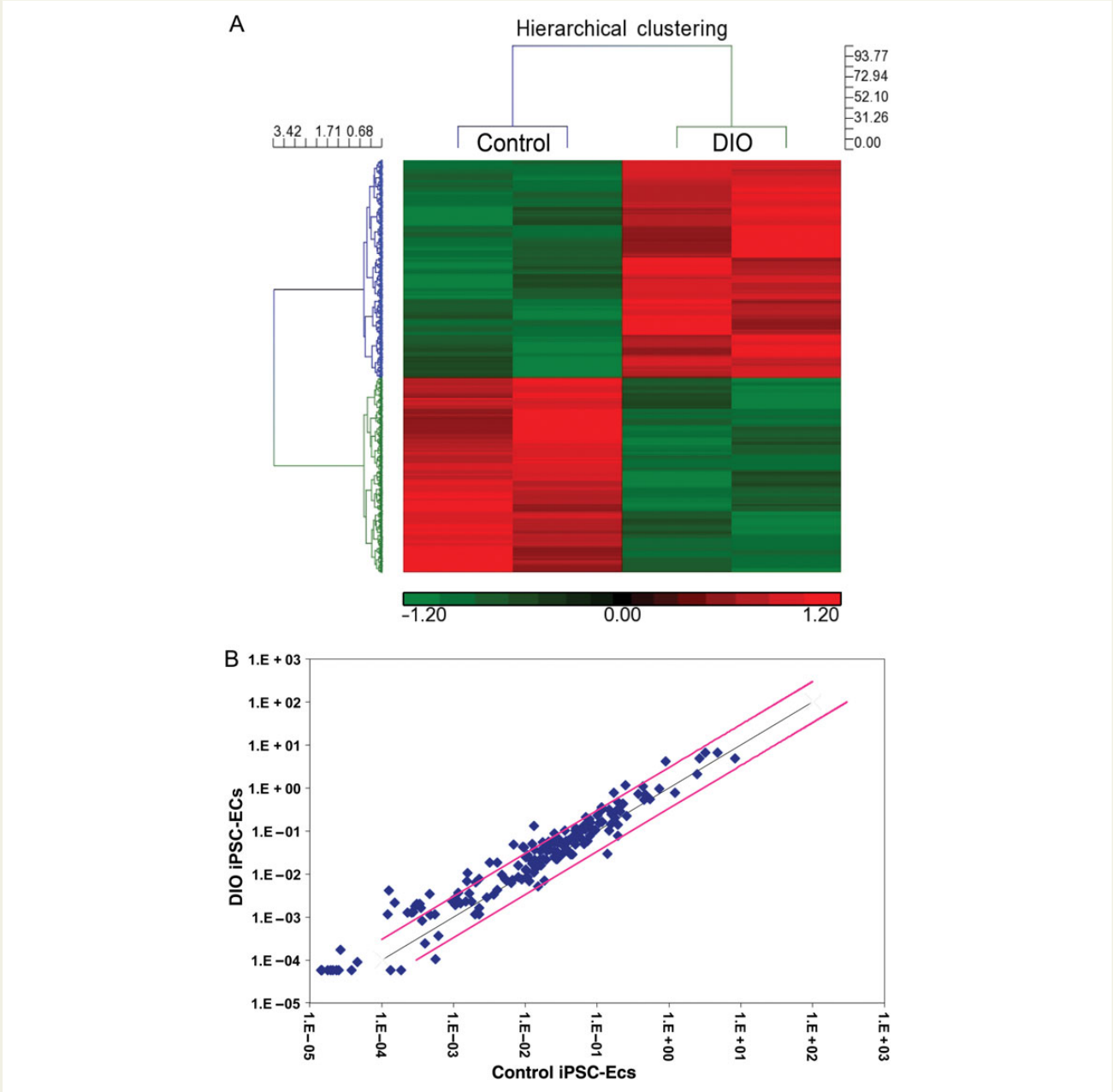


**Figure 4** Microarray and RT-PCR gene expression profiling of induced pluripotent stem cell-derived endothelial cells from control and diet-induced obesity mice. (*A*) Heat map of the 472 significantly differentially regulated genes between diet-induced obesity induced pluripotent stem cell-derived endothelial cells and control induced pluripotent stem cell-derived endothelial cells. Enriched pathway analysis identified the involvement of biological pathways including metabolism, cell cycle, immune function, inflammation, cell adhesion, oxidative stress, senescence, and apoptosis. (*B*) RT-PCR for a panel of genes involved in apoptosis and cellular oxidative demonstrated a significant increase in many of these genes in diet-induced obesity induced pluripotent stem cell-derived endothelial cells compared with control induced pluripotent stem cell-derived endothelial cells ($n = 5$/group). Data expressed as fold-change with the black line indicating a one-fold-change and pink line indicating a three-fold change.

## Activation of Akt-endothelial nitric oxide synthase signalling pathway is suppressed in diet-induced obesity induced pluripotent stem cell-derived endothelial cells

As shown in *Figure 3G*, a hallmark of DIO iPSC-EC dysfunction was reduced NO production, which could be caused by reduced expression of endothelial or cytokine-inducible forms of NO synthase (eNOS and iNOS), impairment of eNOS activation, and/or increased eNOS uncoupling.[18,19] Previous studies have shown that statins can rapidly promote the activation of Akt in endothelial cells leading to eNOS phosphorylation and increased NO production.[20] To address our hypothesis that Akt and eNOS activation by statins was involved in improvement of DIO iPSC-EC function, we assessed eNOS and iNOS gene expressions as well as protein levels in control iPSC-ECs, DIO iPSC-ECs, and DIO iPSC-ECs with pravastatin pre-incubation. We found that DIO iPSC-ECs had significantly lower

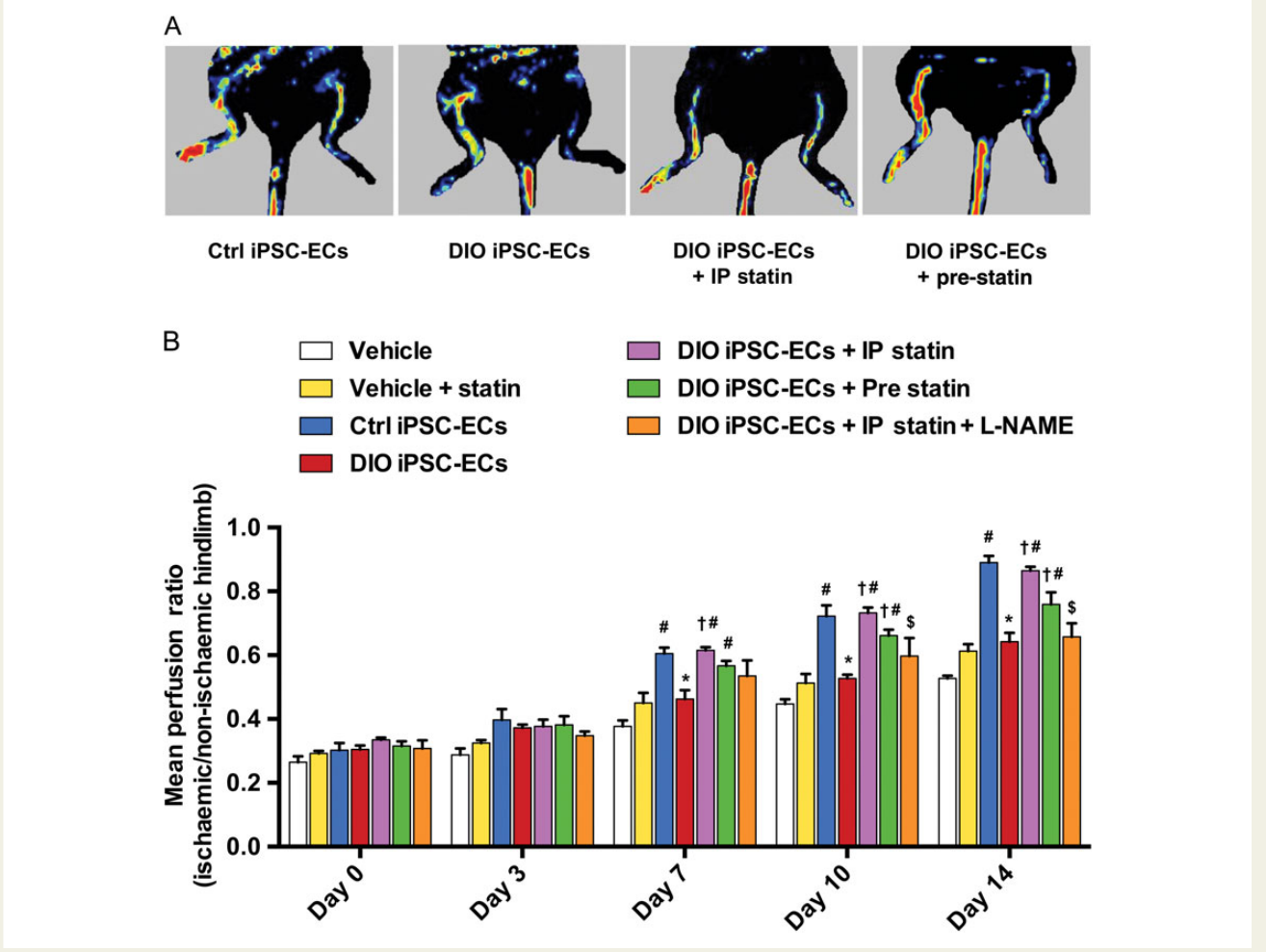


**Figure 5** Laser Doppler imaging of ischaemic hindlimbs following intramuscular injection with vehicle, control induced pluripotent stem cell-derived endothelial cells, diet-induced obesity induced pluripotent stem cell-derived endothelial cells, and diet-induced obesity induced pluripotent stem cell-derived endothelial cells with treatments. (*A*) Graphic representation and (*B*) quantification by laser Doppler imaging show a significant increase in perfusion in the affected hindlimbs of mice injected with $1 \times 10^6$ control induced pluripotent stem cell-derived endothelial cells compared with vehicle alone and vehicle plus statin beginning at Day 7 post-injection ($P < 0.001$ vehicle vs. Ctrl induced pluripotent stem cell-derived endothelial cells; $P = 0.001$ vehicle + statin vs. Ctrl induced pluripotent stem cell-derived endothelial cells). Mice injected with $1 \times 10^6$ diet-induced obesity induced pluripotent stem cell-derived endothelial cells had a significant reduction in hindlimb perfusion compared with mice injected with control induced pluripotent stem cell-derived endothelial cells beginning at Day 7 post-injection ($P = 0.002$). Co-administration of pravastatin 20 mg/kg via daily intraperitoneal injections resulted in a significant increase in hindlimb reperfusion in mice that received diet-induced obesity induced pluripotent stem cell-derived endothelial cells starting from Day 7 ($P < 0.001$), while co-administration of $N^{\omega}$-nitro-L-arginine methyl ester in these mice blocked this effect ($P = 0.004$). Injection with diet-induced obesity induced pluripotent stem cell-derived endothelial cells pre-treated with pravastatin *in vitro* also resulted in a significant increase in hindlimb reperfusion compared with injection of untreated diet-induced obesity induced pluripotent stem cell-derived endothelial cells starting from Day 10 ($P = 0.004$). $n = 10$/group, '†' vs. diet-induced obesity induced pluripotent stem cell-derived endothelial cells, "#" vs. vehicle + statin, "*" vs. control induced pluripotent stem cell-derived endothelial cells, "$" vs. diet-induced obesity induced pluripotent stem cell-derived endothelial cells + intraperitoneal statin.

eNOS expression compared with control iPSC-ECs, which was reversed by pravastatin treatment for 24 h (Supplementary material online, *Figure S6A* and B). Compared with eNOS expression, iNOS gene expression and protein levels were much lower in both control and DIO iPSC-ECs, suggesting a less important role in regulation of endothelial function (Supplementary material online, *Figure S7*). We next assessed the modulation of Akt phosphorylation, eNOS phosphorylation, and eNOS coupling status by western blot analysis. A previous study showed that PKC signalling in endothelial cells inhibits eNOS activity by phosphorylating Thr-495 and dephosphorylating Ser-1177, whereas PKA signalling acts in reverse by increasing phosphorylation of Ser-1177 and dephosphorylation of Thr-495 to activate eNOS.[21] We found that iPSC-ECs from DIO mice showed significantly decreased phospho-Akt and phosphorylation of eNOS at the Ser1177 residue, which was reversed by pravastatin treatment. In contrast, the phosphorylation of eNOS at the Thr495 residue in DIO iPSC-ECs was significantly increased compared with control iPSC-ECs, indicating the deactivation of eNOS is associated with DIO (Supplementary material online, *Figure S6A, C–E*). Finally, the percentage of the dimer-to-monomer ratio, an indicator of eNOS uncoupling which could lead to reduction of enzymatic activity,[22,23] also showed a significant decrease in DIO iPSC-ECs, and was increased by pravastatin treatment (Supplementary material online, *Figure S6A, F*).

## Elevated apoptotic, inflammatory, and oxidative stress pathways in diet-induced obesity induced pluripotent stem cell-derived endothelial cells

Previous studies have shown endothelial dysfunction in patients with obesity is in part related to increased levels of oxidative stress, inflammation, cell apoptosis, and decreased NO production.[24] In order to investigate the mechanisms underlying the *in vitro* functional

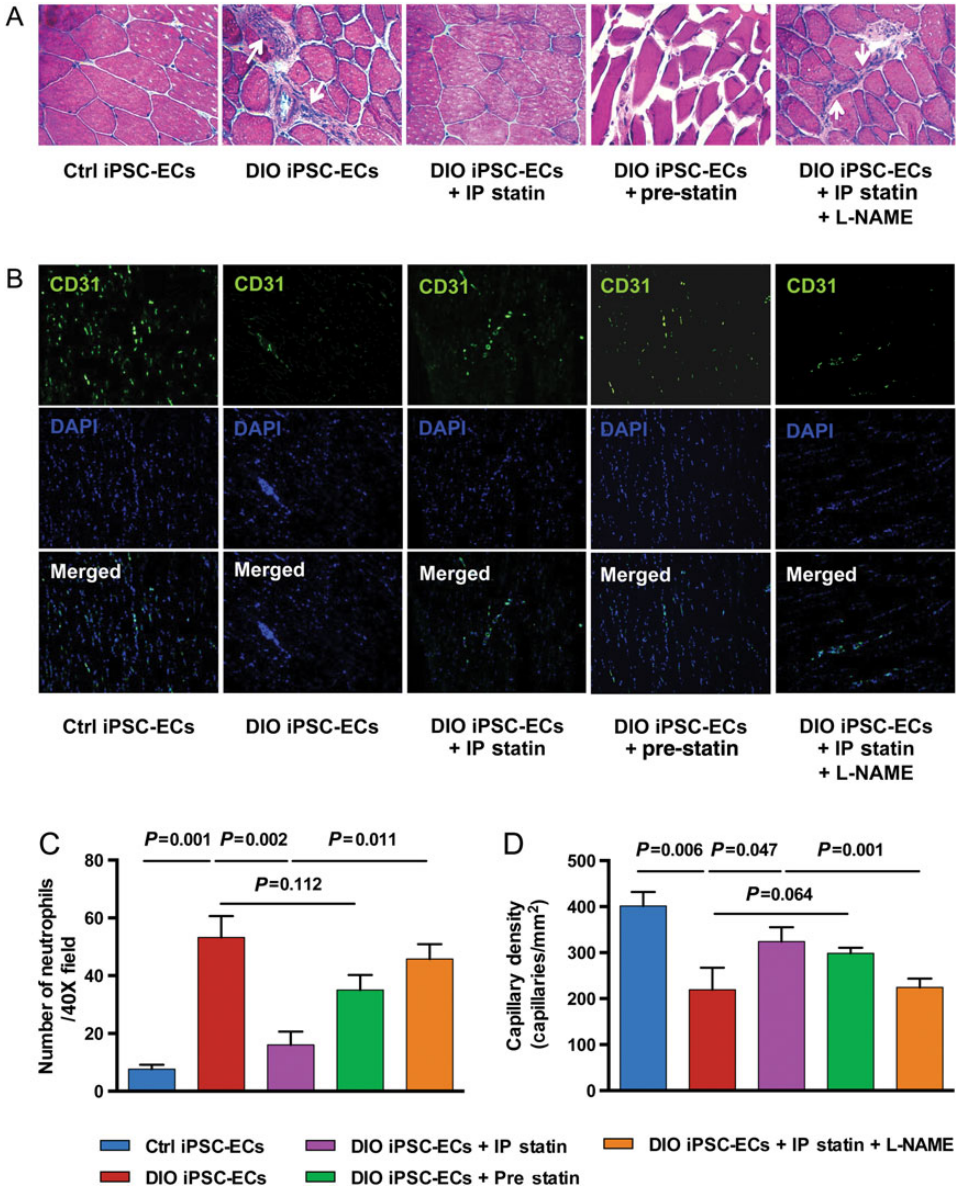

differences observed between DIO iPSC-ECs and control iPSC-ECs, we next performed microarray analysis. Our results indicate that 472 genes were differentially regulated in pathways related to apoptosis, inflammation, oxidative stress, and cellular senescence (*Figure 4A*; Supplementary material online, *Figure S8* and Excel file). We performed RT-PCR on a panel of genes involved in apoptosis and oxidative stress in control iPSC-ECs, DIO iPSC-ECs, and DIO iPSC-ECs after 1 μM pravastatin treatment for 24 h. Of the genes investigated in these panels, 33 were significantly up-regulated (>three-fold) in DIO iPSC-ECs when compared with control iPSC-ECs (*Figure 4B*; Supplementary material online, *Table S2A* and *B*). After pravastatin treatment, 28 apoptotic and oxidative genes were down-regulated in DIO iPSC-ECs. We next performed ELISA assays to determine levels of pro- and anti-inflammatory cytokines in cell culture supernatants following hypoxia for 24 h to mimic an ischaemic environment. Compared with control iPSC-ECs, DIO iPSC-ECs had significantly higher levels of inflammatory cytokines, including IL-1α, IL-1β, IL-4, IFN-γ, and TNF-α. Similarly, incubation of DIO iPSC-ECs with 1 μM pravastatin for 24 h resulted in significant decreases in the pro-inflammatory cytokines IL-1α, IL-1β, IL-4, and TNF-α, as well as significant increases in the anti-inflammatory cytokines IL-6, IL-10, and IL-17A (Supplementary material online, *Figure S9*).

## Dysfunction of diet-induced obesity induced pluripotent stem cell-derived endothelial cells in a hindlimb ischaemia model is reversed by pravastatin co-administration

Several groups have demonstrated that healthy iPSC-ECs are effective in promoting angiogenesis and neovascularization in a hindlimb ischaemia model.[25,26] However, it is unknown if DIO iPSC-ECs will also function properly *in vivo*. To characterize the functional differences between iPSC-ECs from control and DIO mice, we next induced hindlimb ischaemia and used LDI to quantify perfusion. Mice were randomized into seven groups ($n = 10$ per group) and each was administered a single gastrocnemius IM injection of a different treatment regimen (see Supplementary material online). Beginning at Day 7 post-surgery, mice injected with control iPSC-ECs showed a significant increase in hindlimb reperfusion compared with mice injected with vehicle ($0.38 \pm 0.04$ vs. $0.61 \pm 0.04$, vehicle vs. Ctrl iPSC-ECs, $P < 0.001$) or pravastatin only ($0.45 \pm 0.06$ vs. $0.61 \pm 0.04$, vehicle + statin vs. Ctrl iPSC-ECs, $P = 0.001$) (*Figure 5A* and *B*). However, animals injected with DIO iPSC-ECs achieved significantly less hindlimb reperfusion compared with animals injected with control iPSC-ECs ($0.61 \pm 0.04$ vs. $0.46 \pm 0.06$, Ctrl iPSC-ECs vs. DIO iPSC-ECs, $P = 0.002$). In addition, mice randomized to receive DIO iPSC-ECs combined with daily IP administration of pravastatin (beginning at Day 7) and mice randomized to receive DIO iPSC-ECs pre-incubated with pravastatin (beginning at Day 10) both had significantly higher levels of hindlimb reperfusion compared with mice that received DIO iPSC-ECs alone (Day 7: $0.62 \pm 0.02$ vs. $0.46 \pm 0.06$, DIO iPSC-ECs + IP statin vs. DIO iPSC-ECs, $P < 0.001$; Day 10: $0.66 \pm 0.04$ vs. $0.53 \pm 0.02$, DIO iPSC-ECs + pre statin vs. DIO iPSC-ECs, $P = 0.004$), and the level of perfusion was similar to that of mice receiving control iPSC-ECs. When mice that received DIO iPSC-ECs plus daily pravastatin also received the NO synthase inhibitor L-NAME in their drinking water, the increases in hindlimb reperfusion were significantly blunted from Day 7 onwards ($0.62 \pm 0.02$ vs. $0.54 \pm 0.09$, DIO iPSC-ECs + IP statin vs. DIO iPSC-ECs + statin + L-NAME, $P = 0.004$), suggesting that the effect of pravastatin was via an NO-dependent pathway. Finally, we found that starting at Day 7, mice that received DIO iPSC-ECs combined with pravastatin treatment (either systemic

**Figure 6** Histological evaluation of transplanted induced pluripotent stem cell-derived endothelial cells in the ischaemic hindlimb at Day 14. (*A*) H&E staining revealed evidence of muscle degeneration and inflammatory cell infiltration (indicated by white arrows) in animals injected with diet-induced obesity induced pluripotent stem cell-derived endothelial cells compared with animals injected with control induced pluripotent stem cell-derived endothelial cells, whereas animals injected with diet-induced obesity induced pluripotent stem cell-derived endothelial cells with intraperitoneal pravastatin treatment were protected from this damage. Co-administration of the nitric oxide inhibitor $N^{\omega}$-nitro-L-arginine methyl ester blocked the effect of pravastatin in mice receiving diet-induced obesity induced pluripotent stem cell-derived endothelial cells (images at 40×). (*B*) Representative images of hindlimb frozen sections stained with mouse CD31 antibody. (*C*) Infiltration of the inflammatory cells was quantified by counting the number of neutrophils per high power field (40×). Three fields/animal and $n = 5$ animals per group were counted. Mice receiving diet-induced obesity induced pluripotent stem cell-derived endothelial cells showed significantly more neutrophil infiltration compared with mice injected with control induced pluripotent stem cell-derived endothelial cells ($8 \pm 2$ vs. $54 \pm 8$, Ctrl induced pluripotent stem cell-derived endothelial cells vs. diet-induced obesity induced pluripotent stem cell-derived endothelial cells, $P = 0.001$), which was reversed by co-administration of diet-induced obesity induced pluripotent stem cell-derived endothelial cells and intraperitoneal pravastatin ($54 \pm 8$ vs. $17 \pm 5$, diet-induced obesity induced pluripotent stem cell-derived endothelial cells vs. diet-induced obesity induced pluripotent stem cell-derived endothelial cells + intraperitoneal statin, $P = 0.002$). When mice that received diet-induced obesity induced pluripotent stem cell-derived endothelial cells plus daily pravastatin also received the nitric oxide synthase inhibitor $N^{\omega}$-nitro-L-arginine methyl ester in their drinking water, the decrease in neutrophil infiltration was significantly blunted ($17 \pm 5$ vs. $44 \pm 5$, diet-induced obesity induced pluripotent stem cell-derived endothelial cells + intraperitoneal statin vs. diet-induced obesity induced pluripotent stem cell-derived endothelial cells + intraperitoneal statin + $N^{\omega}$-nitro-L-arginine methyl ester, $P = 0.011$). (*D*) Quantification of $CD31^{+}$ staining showed decreased number of capillaries per high power field in the hindlimbs of mice receiving diet-induced obesity induced pluripotent stem cell-derived endothelial cells compared with mice receiving control induced pluripotent stem cell-derived endothelial cells ($P = 0.006$). Co-administration of diet-induced obesity induced pluripotent stem cell-derived endothelial cells with pravastatin for 14 days resulted in a significant increase in capillary density compared with diet-induced obesity induced pluripotent stem cell-derived endothelial cells alone ($P = 0.047$), while co-administration of pravastatin with $N^{\omega}$-nitro-L-arginine methyl ester blocked the effect of pravastatin in animals administered diet-induced obesity induced pluripotent stem cell-derived endothelial cells ($P = 0.001$).

treatment or pre-incubation) showed better hindlimb reperfusion than mice receiving pravastatin alone (0.45 ± 0.06 vs. 0.62 ± 0.02, vehicle + statin vs. DIO iPSC-ECs + IP statin, $P < 0.001$; 0.45 ± 0.06 vs. 0.57 ± 0.03, vehicle + statin vs. DIO iPSC-ECs + pre statin, $P = 0.019$), confirming the necessity of co-administration of pravastatin with DIO iPSC-ECs.

## Histological evaluation of ischaemic hindlimbs confirms an apoptotic and inflammatory phenotype

We next performed histological evaluation of the ischaemic hindlimbs on Day 14 following cell injections. Hematoxylin & eosin (H&E) stained sections of hindlimbs from mice injected with DIO iPSC-ECs showed evidence of muscle atrophy and degeneration, as well as infiltration of inflammatory cells. In contrast, animals injected with control iPSC-ECs or DIO iPSC-ECs plus daily IP injections of pravastatin were protected from this damage. Animals injected with pre-treated DIO iPSC-ECs also showed reduced infiltration of neutrophils; however, the difference between DIO iPSC-ECs and DIO iPSC-ECs pre-treated with pravastatin did not reach statistical significance ($P = 0.112$) (*Figure 6A* and *C*). Immunostaining revealed that $CD31^+$ capillary density was significantly lower in the hindlimbs of mice injected with DIO iPSC-ECs compared with control iPSC-ECs ($P = 0.006$) (*Figure 6B* and *D*). Increased $CD31^+$ capillary density was observed in mice injected with DIO iPSC-ECs plus daily IP injections of pravastatin compared with mice injected with DIO iPSC-ECs alone ($P = 0.047$). Co-administration of the NO synthase inhibitor L-NAME with pravastatin blocked this effect ($P = 0.001$). Moreover, there was a trend showing that injection of DIO iPSC-ECs pre-treated with pravastatin for 7 days could also increase the capillary density compared with injection of untreated DIO iPSC-ECs; however, this did not reach statistical significance ($P = 0.064$). Immunofluorescent staining for CM-DiI-labelled iPSC-ECs verified engraftment of control iPSC-ECs in the ischaemic hindlimbs at Day 14 (Supplementary material online, *Figure S10*). There was less detectable fluorescent signal in sectioned ischaemic hindlimbs of mice injected with labelled DIO iPSC-ECs compared with mice injected with DIO iPSC-ECs combined with daily IP injections of pravastatin.

# Discussion

Following hindlimb ischaemia injury, transplantation of ESC-ECs or iPSC-ECs can result in their incorporation into the host vasculature and increase reperfusion.[9,10,27] However, since cells used in these studies were derived from healthy donors, it remains unknown if iPSC-ECs derived from DIO donors will function in the same way. Since patients who will require intervention to restore normal perfusion are likely to have significant morbidity such as obesity, identifying, and reversing endothelial dysfunction would be important before future application in regenerative medicine.

The current study is the first to compare the functional capacity of iPSC-ECs from control healthy mice vs. DIO mice *in vitro* and *in vivo*. We first showed that DIO iPSC-ECs had impaired function *in vitro* compared with control iPSC-ECs. DIO iPSC-ECs had a reduced capacity to form cord-like structures on Matrigel after 24 h, as well as decreased migration and proliferation *in vitro*. When cultured in hypoxic conditions, DIO iPSC-ECs showed an increase in apoptosis compared with control iPSC-ECs. Second, by using a murine hindlimb ischaemia model, we showed that DIO iPSC-ECs exhibit impaired vascular function *in vivo*. Mice injected with DIO iPSC-ECs achieved significantly less reperfusion beginning at Day 10 compared with mice injected with control iPSC-ECs. While inflammation is often observed following surgical induction of hindlimb ischaemia,[28] we observed significantly more inflammatory cells as well as muscle atrophy in mice injected with DIO iPSC-ECs compared with those injected with control iPSC-ECs. Immunostaining for $CD31^+$ cells also revealed significantly lower capillary density counts in the hindlimbs of mice injected with DIO iPSC-ECs compared with control iPSC-ECs. Microarray gene expression analysis comparing iPSC-ECs from control and DIO mice revealed 472 differentially regulated genes involved in biological pathways, including apoptosis, inflammation, immune function, oxidative stress, and cell senescence.

Previous studies have demonstrated that statin treatment can promote angiogenesis in murine models of hindlimb ischaemia.[20,29] In addition to their lipid lowering effects, statins can decrease inflammation and increase eNOS expression, resulting in a subsequent increase in NO bioavailability.[30–33] In keeping with these observations, another important finding of this study is that co-administration of low-dose pravastatin is able to reverse much of the dysfunction observed with DIO iPSC-ECs both *in vitro* and *in vivo*. Mechanistically, pravastatin therapy had significant beneficial effects *in vitro* on apoptosis, inflammation, and oxidative stress in DIO iPSC-ECs (Supplementary material online, *Figure S11*). Pravastatin also resulted in a significant improvement in hindlimb reperfusion following ischaemia compared with mice receiving iPSC-ECs without pravastatin co-administration. These effects were inhibited by concurrent administration of L-NAME, an NO synthase inhibitor, suggesting the effects of pravastatin were via an NO-dependent mechanism.

Taken together, these results correlate with a large body of evidence demonstrating that in pre-diabetes and DIO, abnormally high levels of inflammatory and oxidative stress biomarkers are associated with increased cellular apoptosis, leading to subsequent long-term complications such as endothelial dysfunction.[34] These prolonged periods of heightened oxidative stress and inflammation can result in dysfunctional progenitor and stem cell populations, which have been implicated in increased risk of cardiovascular disease and PVD in patients with diabetes.[35,36] The observation that DIO iPSC-ECs show impaired function both *in vitro* and *in vivo* suggests one of the consequences of the altered metabolic state is the induction of global epigenetic changes that contribute to impaired EC function seen in these animals. These results are relevant and significant for cell therapy approaches. While autologous iPSC-ECs derived from obese patients might obviate issues associated with immunological rejection, these iPSC-ECs may be inadequate for restoring normal vascular function compared with iPSC-ECs derived from healthy donors. Based on these results, low-dose statin therapy may be a useful adjuvant when co-administered with dysfunctional DIO iPSC-ECs. Finally, the current iPSC-EC platform can also be used to identify additional novel drug targets that can alter the diabetes-induced dysfunctional state.[37]

In summary, our study is the first to show that iPSC-ECs derived from DIO mice exhibit decreased vascular function *in vitro*, and

reduced function and incorporation into the host vasculature *in vivo*. Histological evaluation revealed muscle atrophy and increased infiltration of inflammatory cells in the ischaemic hindlimbs of mice receiving DIO iPSC-ECs. The EC dysfunction may be related to apoptosis, inflammation, and oxidative stress due to decreased NO production. Co-administration with low-dose pravastatin therapy reversed EC dysfunction both *in vitro* and *in vivo*. Collectively, these findings may have important implications and caveats for future patient-specific iPSC-EC therapy, especially in pre-diabetic or DIO patients with PVD.

# Supplementary Material

Supplementary Material is available at *European Heart Journal* online.

## Acknowledgement

We thank B. Wu for critical reading of the manuscript.

## Funding

Financial support from the National Institutes of Health (NIH) T32 EB009035 (N.M.M.), NIH HL107393, NIH U01 HL099776, NIH R01 HL113006, NIH P01 GM099130, AHA Established Investigator Award 14420025, and Fondation Leducq 11CVD02 (J.C.W.).

**Conflict of interest:** J.C.W. is co-founder of Stem Cell Theranostics.

## References

1. Birse RT, Choi J, Reardon K, Rodriguez J, Graham S, Diop S, Ocorr K, Bodmer R, Oldham S. High-fat-diet-induced obesity and heart dysfunction are regulated by the TOR pathway in Drosophila. *Cell Metab* 2010;**12**:533–544.
2. Szendroedi J, Roden M. Ectopic lipids and organ function. *Curr Opin Lipidol* 2009; **20**:50–56.
3. Flegal KM, Carroll MD, Ogden CL, Curtin LR. Prevalence and trends in obesity among US adults, 1999–2008. *JAMA* 2010;**303**:235–241.
4. Du X, Edelstein D, Obici S, Higham N, Zou MH, Brownlee M. Insulin resistance reduces arterial prostacyclin synthase and eNOS activities by increasing endothelial fatty acid oxidation. *J Clin Invest* 2006;**116**:1071–1080.
5. Galassetti P. Inflammation and oxidative stress in obesity, metabolic syndrome, and diabetes. *Exp Diabetes Res* 2012;**2012**:943706.
6. Esposito K, Nappo F, Marfella R, Giugliano G, Giugliano F, Ciotola M, Quagliaro L, Ceriello A, Giugliano D. Inflammatory cytokine concentrations are acutely increased by hyperglycemia in humans: role of oxidative stress. *Circulation* 2002;**106**: 2067–2072.
7. Hink U, Li H, Mollnau H, Oelze M, Matheis E, Hartmann M, Skatchkov M, Thaiss F, Stahl RA, Warnholtz A, Meinertz T, Griendling K, Harrison DG, Forstermann U, Munzel T. Mechanisms underlying endothelial dysfunction in diabetes mellitus. *Circ Res* 2001;**88**:E14–E22.
8. Liu Y, Wei J, Hu S, Hu L. Beneficial effects of statins on endothelial progenitor cells. *Am J Med Sci* 2012;**344**:220–226.
9. Cho SW, Moon SH, Lee SH, Kang SW, Kim J, Lim JM, Kim HS, Kim BS, Chung HM. Improvement of postnatal neovascularization by human embryonic stem cell derived endothelial-like cell transplantation in a mouse model of hindlimb ischemia. *Circulation* 2007;**116**:2409–2419.
10. Yu J, Huang NF, Wilson KD, Velotta JB, Huang M, Li Z, Lee A, Robbins RC, Cooke JP, Wu JC. nAChRs mediate human embryonic stem cell-derived endothelial cells: proliferation, apoptosis, and angiogenesis. *PLoS One* 2009;**4**:e7040.
11. Li Z, Wu JC, Sheikh AY, Kraft D, Cao F, Xie X, Patel M, Gambhir SS, Robbins RC, Cooke JP, Wu JC. Differentiation, survival, and function of embryonic stem cell derived endothelial cells for ischemic heart disease. *Circulation* 2007; **116**(11 Suppl.):I46–I54.
12. Takahashi K, Tanabe K, Ohnuki M, Narita M, Ichisaka T, Tomoda K, Yamanaka S. Induction of pluripotent stem cells from adult human fibroblasts by defined factors. *Cell* 2007;**131**:861–872.
13. Limbourg A, Korff T, Napp LC, Schaper W, Drexler H, Limbourg FP. Evaluation of postnatal arteriogenesis and angiogenesis in a mouse model of hind-limb ischemia. *Nat Protoc* 2009;**4**:1737–1746.
14. Weir C, Morel-Kopp MC, Gill A, Tinworth K, Ladd L, Hunyor SN, Ward C. Mesenchymal stem cells: isolation, characterisation and in vivo fluorescent dye tracking. *Heart Lung Circ* 2008;**17**:395–403.
15. Maehr R, Chen S, Snitow M, Ludwig T, Yagasaki L, Goland R, Leibel RL, Melton DA. Generation of pluripotent stem cells from patients with type 1 diabetes. *Proc Natl Acad Sci USA* 2009;**106**:15768–15773.
16. Caballero AE. Endothelial dysfunction in obesity and insulin resistance: a road to diabetes and heart disease. *Obes Res* 2003;**11**:1278–1289.
17. Hamelin BA, Turgeon J. Hydrophilicity/lipophilicity: relevance for the pharmacology and clinical effects of HMG-CoA reductase inhibitors. *Trends Pharmacol Sci* 1998;**19**: 26–37.
18. Guzik TJ, Mussa S, Gastaldi D, Sadowski J, Ratnatunga C, Pillai R, Channon KM. Mechanisms of increased vascular superoxide production in human diabetes mellitus: role of NAD(P)H oxidase and endothelial nitric oxide synthase. *Circulation* 2002; **105**:1656–1662.
19. Sansbury BE, Cummins TD, Tang Y, Hellmann J, Holden CR, Harbeson MA, Chen Y, Patel RP, Spite M, Bhatnagar A, Hill BG. Overexpression of endothelial nitric oxide synthase prevents diet-induced obesity and regulates adipocyte phenotype. *Circ Res* 2012;**111**:1176–1189.
20. Kureishi Y, Luo Z, Shiojima I, Bialik A, Fulton D, Lefer DJ, Sessa WC, Walsh K. The HMG-CoA reductase inhibitor simvastatin activates the protein kinase Akt and promotes angiogenesis in normocholesterolemic animals. *Nat Med* 2000;**6**:1004–1010.
21. Michell BJ, Chen Z, Tiganis T, Stapleton D, Katsis F, Power DA, Sim AT, Kemp BE. Coordinated control of endothelial nitric-oxide synthase phosphorylation by protein kinase C and the cAMP-dependent protein kinase. *J Biol Chem* 2001;**276**: 17625–8.
22. Zou MH, Shi C, Cohen RA. Oxidation of the zinc-thiolate complex and uncoupling of endothelial nitric oxide synthase by peroxynitrite. *J Clin Invest* 2002;**109**:817–826.
23. Rodriguez-Crespo I, Moenne-Loccoz P, Loehr TM, Ortiz de Montellano PR. Endothelial nitric oxide synthase: modulations of the distal heme site produced by progressive N-terminal deletions. *Biochemistry* 1997;**36**:8530–8538.
24. Bruyndonckx L, Hoymans VY, Van Craenenbroeck AH, Vissers DK, Vrints CJ, Ramet J, Conraads VM. Assessment of endothelial dysfunction in childhood obesity and clinical use. *Oxid Med Cell Longev* 2013;**2013**:174782.
25. Huang NF, Niiyama H, Peter C, De A, Natkunam Y, Fleissner F, Li Z, Rollins MD, Wu JC, Gambhir SS, Cooke JP. Embryonic stem cell-derived endothelial cells engraft into the ischemic hindlimb and restore perfusion. *Arterioscler Thromb Vasc Biol* 2010;**30**:984–991.
26. Lai WH, Ho JC, Chan YC, Ng JH, Au KW, Wong LY, Siu CW, Tse HF. Attenuation of hind-limb ischemia in mice with endothelial-like cells derived from different sources of human stem cells. *PLoS ONE* 2013;**8**:e57876.
27. Yamahara K, Sone M, Itoh H, Yamashita JK, Yurugi-Kobayashi T, Homma K, Chao TH, Miyashita K, Park K, Oyamada N, Sawada N, Taura D, Fukunaga Y, Tamura N, Nakao K. Augmentation of neovascularization [corrected] in hindlimb ischemia by combined transplantation of human embryonic stem cells-derived endothelial and mural cells. *PLoS ONE* 2008;**3**:e1666.
28. Silvestre JS, Mallat Z, Tedgui A, Levy BI. Post-ischaemic neovascularization and inflammation. *Cardiovasc Res* 2008;**78**:242–249.
29. Sata M, Nishimatsu H, Suzuki E, Sugiura S, Yoshizumi M, Ouchi Y, Hirata Y, Nagai R. Endothelial nitric oxide synthase is essential for the HMG-CoA reductase inhibitor cerivastatin to promote collateral growth in response to ischemia. *FASEB J* 2001;**15**: 2530–2532.
30. Davignon J. Beneficial cardiovascular pleiotropic effects of statins. *Circulation* 2004; **109**(23 Suppl. 1):III39–III43.
31. Mason RP, Walter MF, Jacob RF. Effects of HMG-CoA reductase inhibitors on endothelial function: role of microdomains and oxidative stress. *Circulation* 2004;**109**(21 Suppl. 1):II34–II41.
32. Ni W, Egashira K, Kataoka C, Kitamoto S, Koyanagi M, Inoue S, Takeshita A. Antiinflammatory and antiarteriosclerotic actions of HMG-CoA reductase inhibitors in a rat model of chronic inhibition of nitric oxide synthesis. *Circ Res* 2001;**89**:415–421.
33. Schonbeck U, Libby P. Inflammation, immunity, and HMG-CoA reductase inhibitors: statins as antiinflammatory agents? *Circulation* 2004;**109**(21 Suppl. 1):II18–II26.
34. van den Oever IA, Raterman HG, Nurmohamed MT, Simsek S. Endothelial dysfunction, inflammation, and apoptosis in diabetes mellitus. *Mediators Inflamm* 2010;**2010**: 792393.
35. Magenta A, Greco S, Capogrossi MC, Gaetano C, Martelli F. Nitric oxide, oxidative stress, and p66Shc interplay in diabetic endothelial dysfunction. *Biomed Res Int* 2014; **2014**:193095.
36. Ohshima M, Li TS, Kubo M, Qin SL, Hamano K. Antioxidant therapy attenuates diabetes-related impairment of bone marrow stem cells. *Circ J* 2009;**73**:162–166.
37. Matsa E, Burridge PW, Wu JC. Human stem cells for modeling heart disease and for drug discovery. *Sci Transl Med* 2014;**6**:239ps6.